Luminescent Dinuclear Copper(I) Complexes Bearing An Imidazolylpyrimidine Bridging Ligand

Chenfei Li,[a] Wenbo Li,[b] Adam F. Henwood,[a] David Hall,[a,c] David B. Cordes,[a] Alexandra M. Z. Slawin,[a] Vincent Lemaur,[c] Yoann Olivier,[c,d] Ifor D. W. Samuel,[b*] Eli Zysman-Colman[a*]*

[a] Organic Semiconductor Centre, EaStCHEM School of Chemistry, University of St. Andrews, St. Andrews, Fife KY16 9ST, U.K. eli.zysman-colman@st-andrews.ac.uk

[b] Organic Semiconductor Centre, SUPA School of Physics and Astronomy, University of St. Andrews, St. Andrews, Fife KY16 9SS, U.K.

[c] Laboratory for Chemistry of Novel Materials, University of Mons, 7000 Mons, Belgium

[d.] Unité de Chimie Physique Théorique et Structurale & Laboratoire de Physique du Solide, Namur Institute of Structured Matter, Université de Namur, Rue de Bruxelles, 61, 5000 Namur, Belgium.

ABSTRACT: The synthesis and the photophysical study of two dinuclear copper(I) complexes bearing a 2-(1*H*-imidazol-2-yl)pyrimidine bridging ligand are described. The tetrahedral coordination sphere of each copper centre is completed through the use of a bulky bisphosphine ligand, either DPEphos or Xantphos. Temperature-dependant photophysical studies demonstrated emission through a combination of phosphorescence and thermally activated delayed fluorescence (TADF) for both complexes, and an intense emission (Φ_{PL} = 46%) was observed for a crystalline sample of one of the complexes reported. The photophysics of these two complexes is very sensitive to the environment. Two pseudopolymorphs of one of the dinuclear complex were isolated, with distinct photophysics. The emission color of the crystals

can be changed by grinding, and the differences in their photophysics before and after grinding are discussed.

Introduction

As a result of the high abundance of copper in the Earth's crust (68 ppm for copper compared with 0.0004 ppm for iridium),[1] copper(I) complexes are considered to be potential candidates for sustainable light emitting materials and as photocatalysts. Moreover, copper(I) complexes possess a d^{10} electronic configuration and thus avoid non-emissive and photodissociative processes associated with the population of d-d states. Their emission energies are easily tunable through ligand modulation due to the metal-to-ligand charge transfer (MLCT) nature of the excited state of most mononuclear copper(I) complexes. In addition, they have long been found to be photoactive and emissive. Indeed photoactive $[Cu(N\hat{}N)(P\hat{}P)]^+$ and $[Cu(N\hat{}N)_2]^+$ types of complexes were first reported by Sakaki *et al*.[2,3] and Sauvage *et al*.,[4] respectively, more than thirty years ago. In 2002, McMillin *et al*.[5] focussed in particular on the luminescence properties of heteroleptic $[Cu(N\hat{}N)(PPh_3)_2]^+$ and $[Cu(N\hat{}N)(DPEPhos)]^+$ (DPEPhos = bis[(2-diphenylphosphino)phenyl] ether) type of complexes. Although there were no devices fabricated in these initial studies, a very long excited state lifetime (τ_{PL} = 14.3 μs) and relatively high photoluminescence quantum yield, Φ_{PL}, of 15% in DCM were found for $[Cu(dmp)(DPEPhos)]BF_4$ (dmp = 2,9-dimethyl-1,10-phenanthroline). Wang *et al*. later reported organic light emitting diodes (OLEDs) fabricated with the related complex $[Cu(dnbp)(DPEPhos)]BF_4$ (dnbp = 2,9-di-*n*-butyl-1,10-phenanthroline), which achieved a current efficiency up to 11.0 cd A^{-1} at a current density of 1.0 mA cm^{-2}.[6] Moreover, this family of complexes has also been used in other applications, For instance, Xiao *et al*. studied the photopolymerization of both acrylates and epoxides using three different $[Cu(N\hat{}N)(P\hat{}P)]^+$ type complexes. The polymerization was initiated by a cation generated from the photoredox

catalytic reaction between an iodonium salt and the Cu(I) photocatalyst while *N*-vinyl-9*H*-carbazole (NVK) was observed to accelerate the reaction. Of the complexes investigated as photocatalysts, [Cu(dmp)(DPEPhos)]BF_4 exhibited the highest reactivity due to the correspondingly large molar extinction coefficient of the Metal Ligand Charge Transfer (MLCT) band.[7]

Although mononuclear heteroleptic copper complexes of the form $[Cu(N^N)(P^P)]^+$, remain arguably the largest and most widely studied family of complexes studied, there is growing interest in dinuclear copper(I) complexes (Figure **1**), with Peters *et al*. reporting the first example of a highly emissive bis(phosphine)diarylamido dinuclear copper(I) complex in 2005 (Figure **1a**). This is in part because the Φ_{PL} values of cuprous dinuclear complexes are generally higher compared to their mononuclear analogues, such as 16% in DCM for $[Cu(dbp)(DPEPhos)]^+$ reported by McMillin *et al*.[5] compared to 67% in THF for $[Cu(PNP)]_2$ reported by Peters *et al*.[8] This has been attributed to a combined effect of steric protection by the bulky $[PNP]^-$ ligand and the absence of a net positive charge in the dinuclear complex. In 2010, Robertson *et al*. reported a dinuclear copper(I) complex containing a bipyrimidyl bridging ligand (**Figure 1b**); however, they failed to purify the complex, and no photophysics data were reported.[9] In 2013, Bräse *et al*. reported a group of iodide-bridged heteroleptic copper(I) complexes.[10] Moderate-to-high photoluminescence quantum yields (36-99%) and long photoluminescence lifetimes of the order of microseconds (1.09-4.22 μs) for the powder samples were observed. All complexes of this group exhibited MLCT (Cu_2I_2 core to P^N ligand) excited states, and the more emissive complexes showed a triplet spin-density distributed across both the Cu_2I_2 core and the P^N ligand, while the less emissive complexes reported showed triplet spin-density localized only on the P^N ligand. OLED devices were fabricated for one of the complexes (Figure **1c**), and a luminance of 1800 cd m^{-2} and a CE_{max} of

8.74 cd A^{-1} was achieved for this blue-green emitting device.[11] De Cola *et al*. reported two $Cu_2(N\hat{}N)_2(P_2\hat{}P_2)$ complexes (Figure **1d**). These complexes showed high Φ_{PL} of up to 49% in MeCN and long τ_{PL} of up to 13.8 μs and were found to show TADF, with one of the dinuclear complexes (Figure **1d**) possessing a small ΔE_{ST} of only 0.02 eV, although the ΔE_{ST} value of the other complex was not reported. Light-emitting electrochemical cells (LEEC) were fabricated and achieved a maximum luminance of 108 cd/m^2.[12] Kato *et al*. reported a group of highly emissive $[Cu_2(N\hat{}P\hat{}N)_2]X_2$ complexes synthesised by mechanochemical methods with powder Φ_{PL} values of up to 74% (Figure **1e**).[13] At room temperature, the powder samples of these complexes exhibited blue to green emission (λ_{PL} from 470 nm to 530 nm) and microsecond τ_{PL}s (5-33 μs) while at 77 K the emission spectra slightly red-shifted by 9-22 nm (39-98 meV) and showed slower emission decay. Green-emissive $Cu_2(N_2\hat{}N_2)(P\hat{}P)_2$ complexes (λ_{PL} ~520 nm, Φ_{PL} range from 29% to 79%) were reported by Lu *et al*., with one of them showing a high Φ_{PL} of 79% (Figure **1f**) in the crystal. These complexes exhibit efficient TADF (ΔE_{ST} ~ 0.1 eV) with relatively fast radiative decay rates (up to 1.4×10^5 s^{-1}) at room temperature. OLEDs using these complexes as emitters showed EQE_{max} values of up to 8.3% and a peak luminance of 2525 cd m^{-2}.[14] Very recently, Yersin *et al*. reported a family of highly luminescent (Φ_{PL} up to 84%) yellow-green-emissive $[Cu_2(\mu\text{-}P\hat{}P)][X_2]$ complexes (Figure **1g**). These materials, identified as showing TADF, had very short delayed lifetimes (as low as 1.2 μs) due to the ΔE_{ST} values being as small as 0.048 eV.[15]

a)

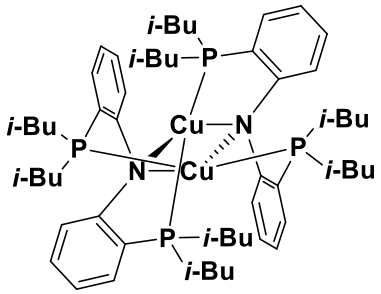

Peters *et al.*
J. Am. Chem. Soc. **2005**, 127, 2030.

b)

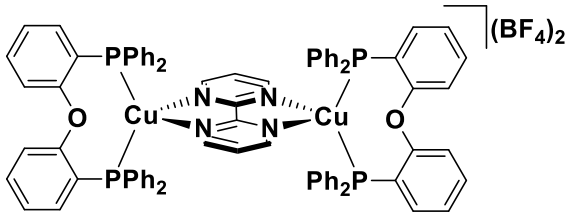

Robertson *et al.*
Dalton. Trans. **2010**, 39, 8945.

c)

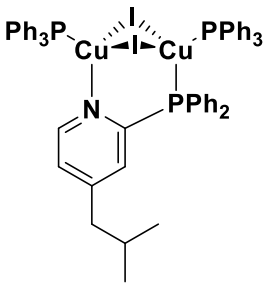

Bräse *et al*.
Chem. Mater. **2013**, 25, 4471.

d)

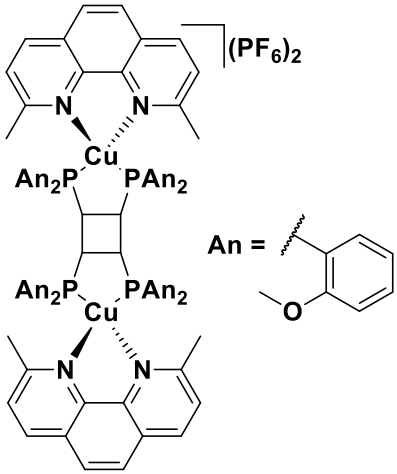

De Cola *et al.*
Inorg. Chem. **2014**, 53, 10944.

e)

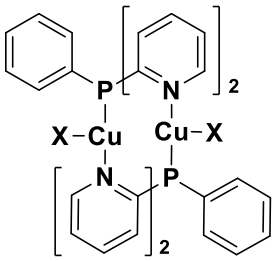

X = Cl, Br, I

Kato *et al.*
Inorg. Chem. **2016**, 55, 1978.

f)

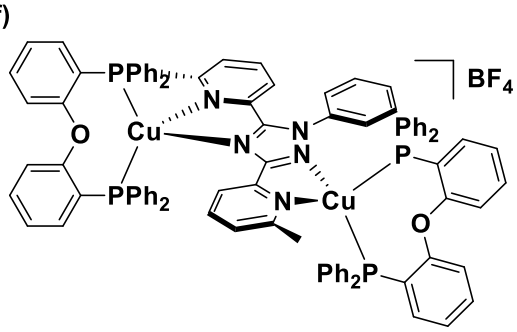

Lu *et al.*
J. Mater. Chem. C **2017**, 5, 4495.

g)

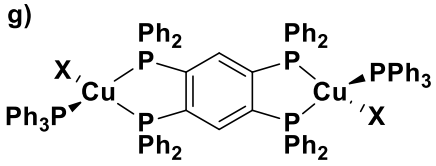

X = Cl, Br, I, NCS

Yersin *et al.*
Chem. Mater. **2019**, 31, 4392.

Figure **1**. Representative examples of dinuclear copper(I) complexes.

Herein, we report two novel $Cu_2(\mu\text{-N^N})(P^P)_2$ complexes bearing 2-(1*H*-imidazol-2-yl)pyrimidine bridging ligand (impymH) as a deprotonated bridging ligand, $[Cu_2(impym)(Xantphos)_2]BF_4$ and $[Cu_2(impym)(DPEPhos)_2]BF_4$ (Scheme **1**). In solution, both complexes exhibited weak blue emission from a ligand-centred (LC) state with nanosecond-long τ_{PL}s. These complexes exhibit aggregation-induced-emission (AIE) where the aggregated nanoparticles showed very bright yellow metal-to-ligand charge-transfer emission. In contrast to other copper(I)[16] and platinum(II)[17,18] complexes showing AIE, we found that in dilute solution the MLCT emission is too weak to be detectable and all that is observed is residual LC emission; however, when the nanoparticles form, the non-radiative decay processes are suppressed and MLCT emission, typically observed for $[Cu(N^N)(P^P)]^+$ complexes, is restored.

Moreover, crystallised samples of $[Cu_2(impym)(Xantphos)_2]BF_4$ revealed two pseudopolymorphic forms that show different emission colors and associated photophysical properties. Upon grinding the crystalline samples of these two pseudopolymorphs, we observed an emission color change as well as a change in the emission intensity, which we assign to a combined effect of losing solvation and conversion of one form into the other during grinding.

Results and Discussion

Synthesis of ligand and complexes

The impymH ligand was prepared in modest yield via the condensation of pyrimidine-2-carbonitrile and 2,2-dimethoxyethan-1-amine.[19] Complexes **D1** and **D2** were then isolated as their tetrafluoroborate salts via crystallization following complexation of impymH with $[Cu(NCMe)_4]BF_4$ and either DPEPhos or Xantphos (Scheme **1**).[20] The identity and purity of the

two complexes were ascertained by a combination of ^{1}H, ^{19}F, ^{31}P, ^{13}C NMR spectroscopies, mass spectrometry and elemental analysis (see Synthesis and characterisation in **ESI**). The structures of both complexes were determined by single crystal X-ray diffraction. Both complexes are soluble and chemically stable in a wide number of organic solvents (*e.g.*, dichloromethane, chloroform, acetone, methanol), as well as being stable under ambient conditions in the solid state as powders.

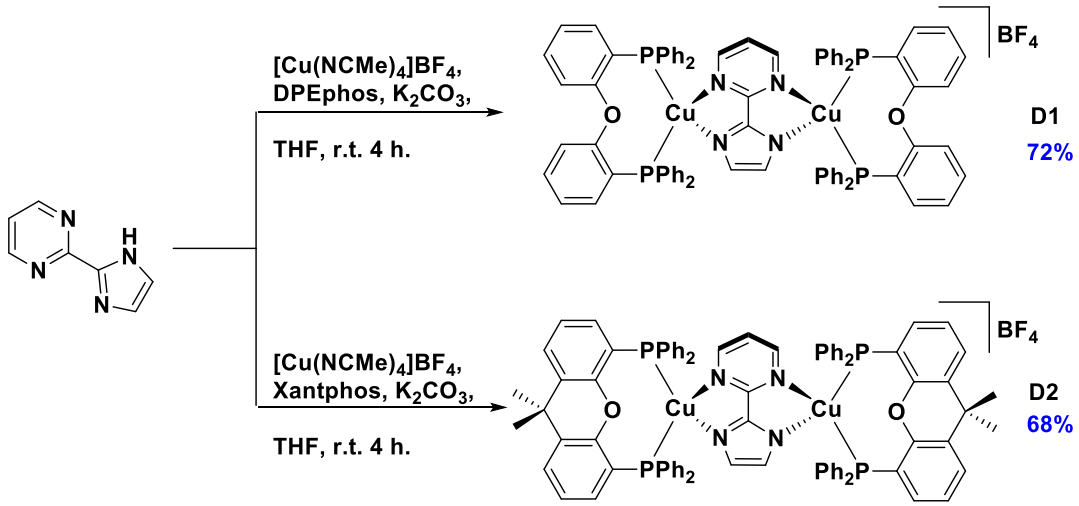

Scheme **1**. Synthesis of homodinuclear complexes.

X-ray crystallography.

Single crystals of **D1** and **D2-a** were obtained by diffusing diethyl ether vapor into concentrated DCM solution of the complex (method 1, ESI), while crystals of **D2-b** were obtained from the slow evaporation of a mixed DCM/methanol solution of **D2** (method 5, ESI). The solid-state structures of each of sample occupy similar or the same monoclinic space groups: $P2_1/c$ for **D1** and **D2-a**, and $P2_1/n$ for **D2-b** (Figure **2**). The crystal structures reveal as expected that each copper atom is tetracoordinated and that the impym ligand acts to bridge the two [Cu(P^P)] fragments. The oxygen atoms of the two DPEPhos or Xantphos ligands in both **D1** and **D2-b** are on opposite sides of the copper–impym-copper plane (Figure **2**) and, therefore, they adopt a *pseudo-trans* configuration. In contrast, **D2-a**, with its Xantphos oxygen

atoms on the same side of the copper–impym-copper plane, adopts a *pseudo-cis* configuration. However, in both **D2** complexes, the Xantphos oxygen atoms are close to the copper–impym-copper plane.

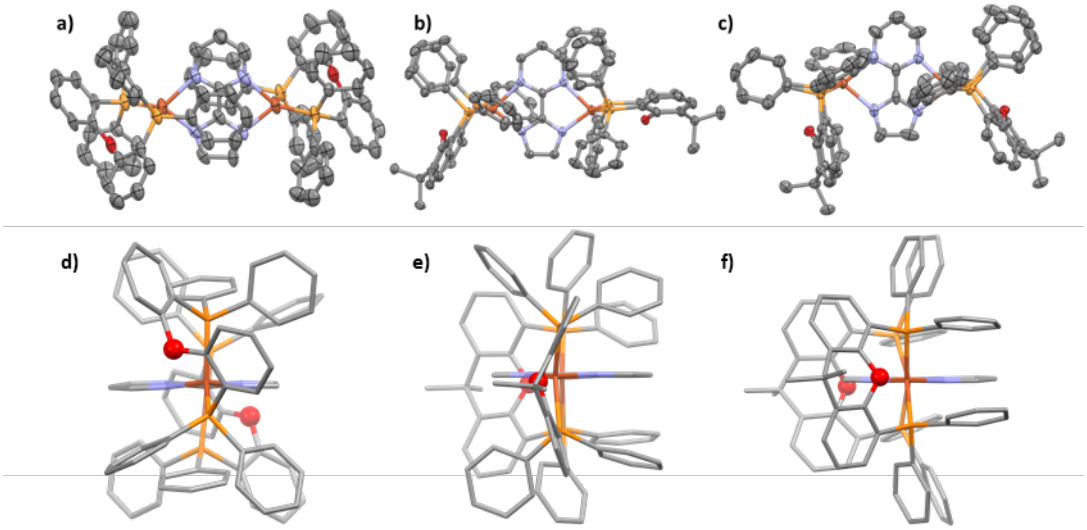

Figure **2**. (top) Thermal ellipsoid plots of the X-ray structures of (a) **D1**, (b) **D2-a** and (c) **D2-b**. Solvent molecules, BF_4^- anions and hydrogen atoms have been omitted for clarity. Ellipsoids are drawn at the 50% probability level. (bottom) Views showing the position of phosphine-ligand oxygens relative to the copper–impym-copper plane (shown as a red line) for (d) *pseudo-trans* **D1**, (e) *pseudo-cis* **D2-a** and (f) *pseudo-trans* **D2-b**.

Selected bond lengths, angles and distances are listed in Table **1**. As expected, the two copper centres in each complex exhibit a tetrahedral geometry. The four N-Cu bonds for each complex are of similar length, implying that the impym ligand coordinates with its negative charge equally distributed to both copper centers rather than coordinating formally datively to one copper center and covalently to the second. Despite the two different bisphosphine ligands used, **D1**, **D2-b** and one P^P ligand of **D2-a** have similar P-Cu-P bite angles, ranging from 114.00(4)° to 117.72(4)°. In contrast, the second bisphosphine ligand in **D2-a** has a P-Cu-P bite angle of 127.74(4). There is one apparent configurational difference between this wide-bite Xantphos, and the other three in **D2-b** and **D2-a**, namely that the xanthine mean plane is

approximately coplanar with the P_4 mean plane, while the other three xanthine mean planes are close to orthogonal to the P_4 mean plane.

Table **1**. Selected bond lengths, bond angles and dihedral angles in **D1**, **D2-b** and **D2-a**.

Lengths (Å)				Angles (°)			
	D1	**D2-b**	**D2-a**		**D1**	**D2-b**	**D2-a**
Average P-Cu bond length	2.25	2.25	2.26	**P-Cu-P bite angles**	115.40(7), 117.39(7)	114.00(4), 117.32(4)	117.72(4), 127.74(4)
Average N-Cu bond length	2.10	2.13	2.12	**Average N-Cu-N angle**	82.1	81.29	81.60
Shortest Cu···Cu distance (intramolecular)	5.4766(11)	5.5521(8)	5.5216(7)	**Torsion angle of N^N ligand**	1.0(9)	1.6(6)	2.2(5)
Shortest Cu···Cu distance (intermolecular)	8.4649(18)	10.2257(9)	9.1209(11)	**Average N^N P^P twsting angle**	86.61	87.69	86.61

UV-Visible absorption spectroscopy

The absorption spectra **D1** and **D2** are shown in Figure **3** and the data compiled in Table **2**. Both complexes absorb light with wavelength shorter than ~ 430 nm ($E_{0,0}$, determined from the intersection point of the normalized emission and absorption spectra, is 3.13 eV for **D1**, 3,12 eV for **D2**). The interpretation of the absorption spectra was carried out in the frame of Time-Dependent-Density Functional Theory using the Tamm-Dancoff (TDA-DFT) approximation.[21] The nature of the excited states was determined thanks the analysis of the hole and electron densities plots. The hole (electron) isosurface plots were generated using the Jmol program[22] by combining for each atom the LCAO coefficients in all occupied (unoccupied) molecular orbitals involved in the one-electron transitions contributing to a given excited state as well as their weights in the TDA-DFT wavefunction.

According to TDA-DFT calculations,[21] the nature of the S_1 excited state for both complexes is a metal-to-ligand charge transfer (MLCT) where the charge transfer terminates at the π-accepting impym ligand, and in particular on the pyrimidine ring. Band II (~350 nm) has mixed MLCT and LLCT (ligand-to-ligand charge transfer) character involving the impym ligand; the charge being transferred from the imidazole unit to the pyrimidine moiety. An intense transition

centered on the impym ligand is calculated at 294 nm (band III) for **D1**. It involves a charge transfer from the imidazole ring to the whole impym ligand ensuring enough overlap between the hole and electron densities. For **D2**, the transition is less intense since the charge transfer, which involves the impym ligand, mainly goes from the imidazole unit to the pyrimidine moiety exhibiting smaller overlap between the hole and electron densities. At higher energies (~280nm, band IV), calculations reveal that the band mainly exhibits a MLCT character; from the metallic centers to the impym and the P^P ligands for **D1** and **D2**, respectively. The UV-Vis spectra of **D1** and **D2** are similar to other dinuclear copper(I) complexes of the general form $Cu_2(\mu\text{-}N\text{^}N)(P\text{^}P)_2$ reported by Lu *et al*.[14] The $Cu_2(N\text{^}N)_2(P_2\text{^}P_2)$ type copper(I) complexes reported by De Cola *et al*.[12] showed red-shifted absorption spectra compared to **D1** and **D2** due to the use of the more π-accepting dmphen ligand, with the lowest energy absorption band assigned to be a purely MLCT transition at 420 nm.

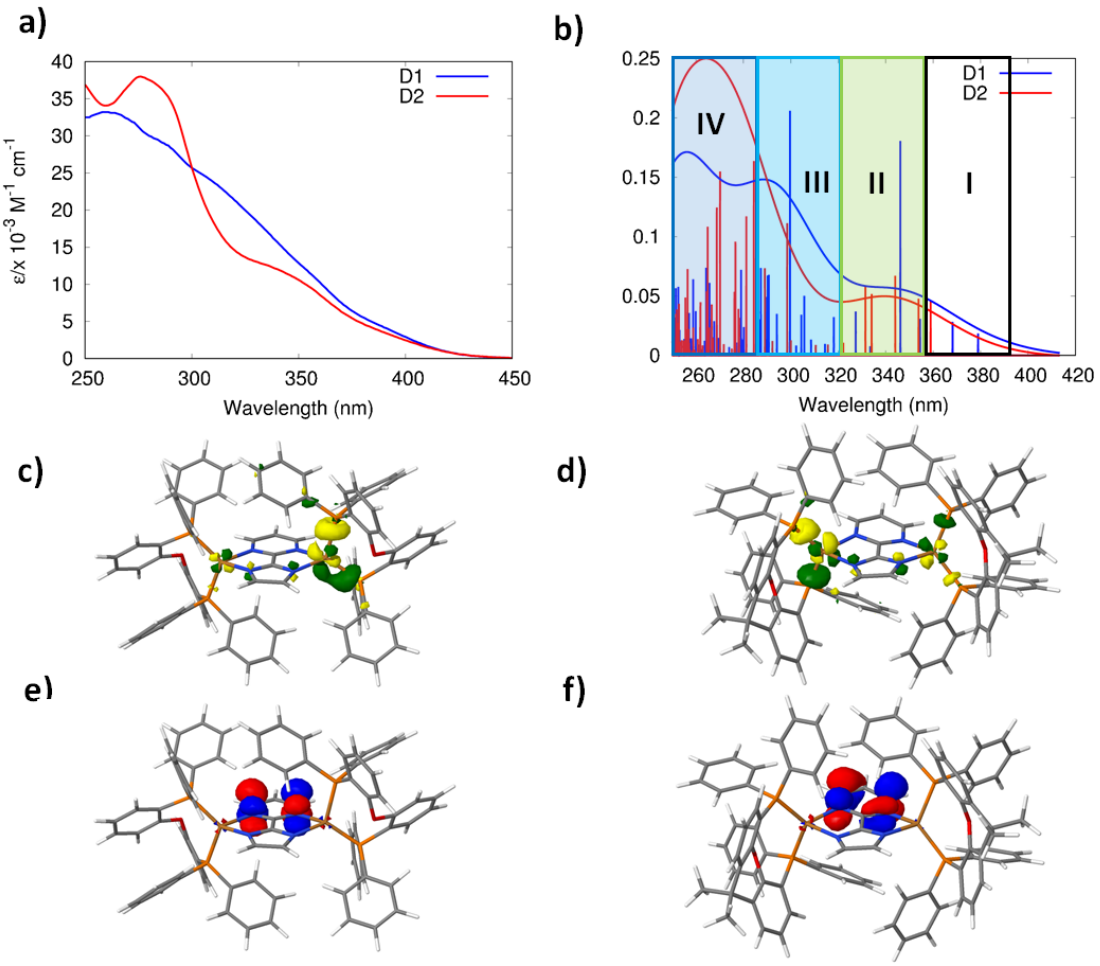

Figure **3**. (a) Experimental and (b) TDA-DFT UV-Vis absorption spectroscopy of **D1** and **D2** including solvent effects in DCM using the Polarizable Continuum Model (PCM). Hole [electron] density isocontour plots for the S_1 excited state of c) [e)] **D1** and d) [f)] **D2**.

Table **2**. Summary of the experimental and predicted UV-Vis absorption spectra.

Complex	Band[a]	λ / nm (ε / × 10^{-3} $M^{-1}cm^{-1}$)[b]	λ / nm (No. of state)	*f*	Character
D1	IV	288 (29)	279(27)	0.07	$MLCT_{(Cu->P^P)}$
			287(18)	0.07	$MLCT_{(Cu->P^P)}$
			290(16)	0.07	$MLCT_{(Cu->N^N(6-R))}$
			290(15)	0.07	$MLCT_{(Cu->N^N(6-R))}$
	III	320 (21)	294(13)	0.20	$LC_{(N^N(5-R)->N^N)}$
	II	352 (12)	346(4)	0.18	$MLCT_{(Cu->N^N)}$
	I	388 (4)	379(1)	0.02	$MLCT_{(Cu->N^N(6-R))}$
D2	IV	277 (38)	269(30)	0.12	$MLCT_{(Cu->P^P)}$
			270(29)	0.15	$MLCT_{(Cu->P^P)}$
			281(19)	0.12	$MLCT_{(Cu->P^P)}$
			284(18)	0.16	$MLCT_{(Cu->P^P)}$ + $LLCT_{(N^N(5-R)->P^P)}$
	III	---	298(13)	0.11	$LC_{(N^N(5-R)->N^N)}$
	II	349 (9)	331(5)	0.06	$MLCT_{(Cu->N^N(6-R))}$ + $LC_{(N^N(5-R)->N^N(6-R))}$
	I	402 (2)	359(1)	0.05	$MLCT/LLCT_{(P^P->N^N)}$

[a]Bands were identified based on TD-DFT calculations; [b]Wavelength corresponds to either a peak or an inflection point associated with each band; 5-R represent imidazole part of bridging ligand while 6-R represent pyrimidine part of bridging ligand

Electrochemical properties

The electrochemical properties of **D1** and **D2** were measured by cyclic voltammetry (CV) in THF (Figure **4**) and the data are listed in Table **3**. Both complexes showed irreversible oxidation and reduction waves. The first oxidation potential of both complexes corresponds to the $Cu^{I/II}$ redox couple with significant P^P character. The oxidation potential of **D2** (E_{pa} = 1.10 V) is slightly anodically shifted compared to that of **D1** (E_{pa} = 1.00 V). Both complexes show a second irreversible oxidation wave (E_{ox} = 1.20 V for **D1** and E_{ox} = 1.31 V for **D2**) that is assigned by DFT calculations (Figure **5**) to the oxidation of the second copper centre, revealing the expected electronic communication between the two metals. There is an irreversible reduction wave at -2.20 V for **D1** and -2.16 V for **D2**, assigned by DFT calculations to the reduction of the pyrimidine ring of the impym ligand; a second reduction wave at -2.42 V is

evident for **D1**, which was assigned to a second reduction of impym ligand. This second reduction wave is not present in **D2**. The HOMO and LUMO energy levels were extrapolated from the CV data (Table **3**). Complex **D2** possesses a slightly deeper HOMO than **D1** (-5.16 eV for **D1**, -5.26 eV for **D2**) while the LUMO of both complexes is at -2.5 eV. The HOMOs of the $[Cu_2(\mu\text{-N^N})(P^P)_2]$ type copper(I) complexes (see Figure **5**) reported by Can-Zhong Lu *et al*.[14] were ~-5.2 eV, close to those measured for **D1** and **D2**, while the LUMOs were at ~-2.3 eV, slightly higher than our complexes, due to the difference in structure of the bridging ligands (pyridyl *vs*. pyrimidyl).

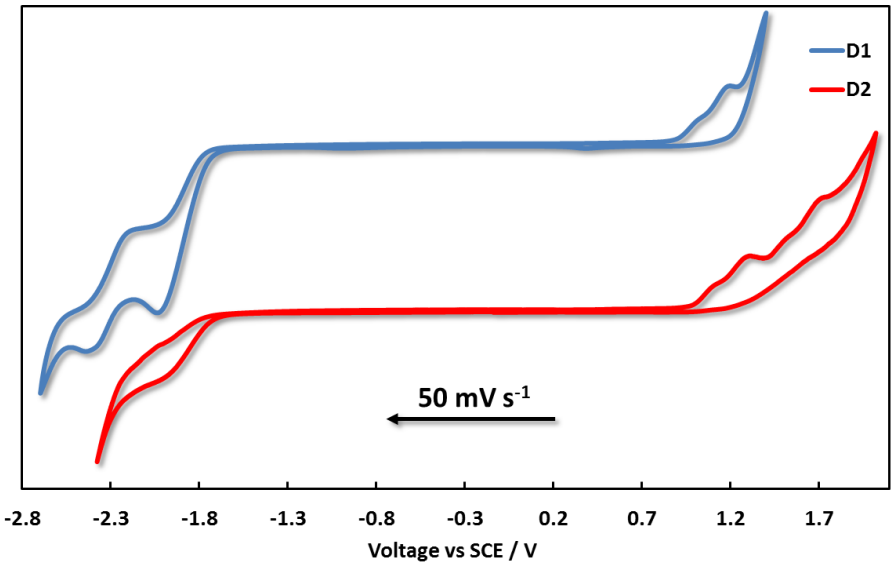

Figure **4**. Cyclic Voltammograms of **D1** and **D2** in THF, Fc/Fc^+ couple (0.56 V *vs*. SCE) was used as internal standard.[23] Working electrode: glassy carbon; reference electrode: silver wire; counter electrode: platinum wire.

Photoactive copper(I) complexes have been used for more than thirty years as photoredox catalysts.[24,25] In order to assess the viability of these two complexes as photoredox catalysts we calculated the excited state redox potentials given an optical gap of 3.13 eV for **D1** and 3.12 eV for **D2**. Both complexes showed very negative excited state oxidation potentials (E^*_{ox} = -2.13 V for **D1** and -2.02 V for **D2**), which are more negative than that of the strong photoreductant *fac*-$Ir(ppy)_3$ (E^*_{ox} = -1.73 V vs SCE in MeCN).[26] Compared to the well-studied

homoleptic copper(I) photocatalyst, $[Cu(dap)_2]Cl$ (E^*_{ox} = -1.43 V vs SCE in MeCN),[27] and heteroleptic copper(I) photocatalyst, [Cu(dmphen)Xantphos]$^+$ (E^*_{ox} = -0.95 V vs SCE in MeCN),[28,29] complexes **D1** and **D2** are significantly more reducing in their excited state. Due to their very negative ground state reduction potentials, the exited state reduction potentials (E^*_{red} = 0.93 V for **D1**, 0.96 V for **D2**) makes these complexes weak photooxidants, about the same as the commonly employed $[Ru(bpy)_3]^{2+}$ (E^*_{red} = 0.77 V vs SCE in MeCN);[30] the reduced complexes are themselves very strong reductants, capable of reducing substrates such as dichloroethane (E_{red} = -1.92 V), benzaldehyde (E_{red} = -1.93 V) or *N*-benzylideneaniline (E_{red} = -1.91 V).[31]

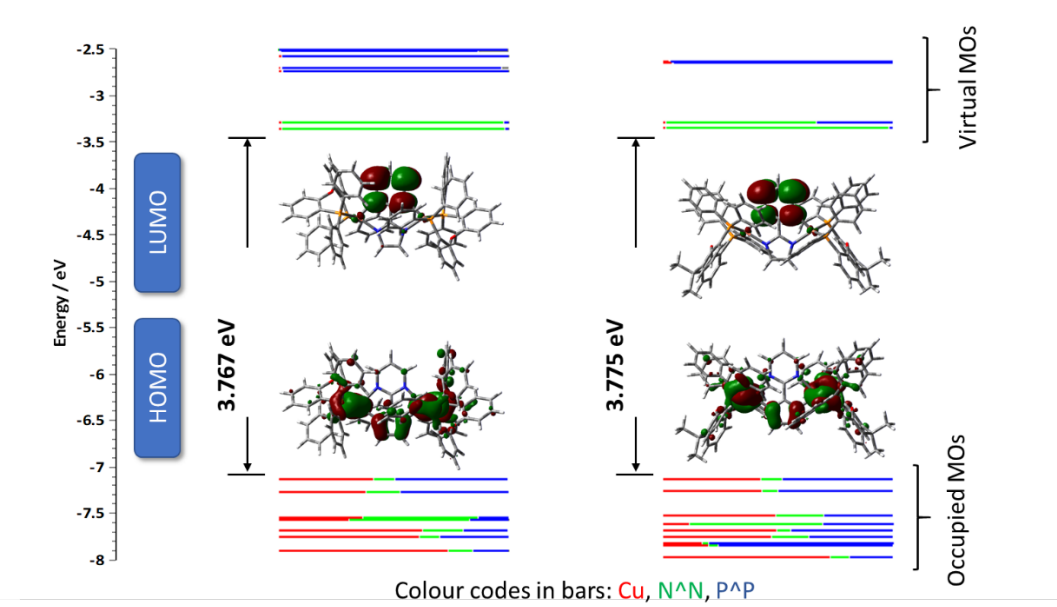

Figure **5**. Calculated Kohn–Sham energy level diagram and electron density distribution images of the HOMO and LUMO of **D1** and **D2**.

Table **3**. Ground and excited state redox properties of **D1** and **D2**.[a]

	E_{ox}/ V	E_{red}/ V	ΔE_{redox}/ V	E^*_{ox}/ V	E^*_{red}/ V	HOMO/ eV	LUMO/ eV	$E_{0,0}$/ eV
D1	1.00	-2.20	3.23	-2.13	0.93	-5.16	-2.50	3.13

D2	1.10	-2.16	3.30	-2.02	0.96	-5.26	-2.51	3.12

[a] Working electrode: glassy carbon; reference electrode: silver wire, counter electrode: platinum wire; solvent: THF; $E_{HOMO} = -(E_{[onset,ox\ vs.\ Fc+/\ Fc]} + 4.8)$ (eV) $E_{LUMO} = -(E_{[onset,red\ vs.\ Fc+/\ Fc]} + 4.8)$ (eV);[32] all redox waves are irreversible, hence, E_{pa} is used for E_{red}, while E_{pc} is used for E_{ox}; excited state redox potential calculated with optical gap from UV-Vis absorption spectra, $E^*_{ox} = E_{ox} - E_{0,0}$, $E^*_{red} = E_{red} + E_{0,0}$.[33,34]

Photophysical properties

The photoluminescence spectra of **D1** and **D2** in DCM at 298 K are shown in Figure **6**. The λ_{PL}s of **D1** and **D2** are 425 and 468 nm, respectively. As with most tetrahedrally coordinated copper(I) complexes, both **D1** and **D2** are poorly emissive in DCM solution. The very low Φ_{PL}s (Φ_{PL} << 1% for both complexes) implies very large non-radiative decay rate constants for both complexes. This is also due to both the small but non-negligible oscillator strengths (0.039 for **D1** and 0.090 for **D2**) computed for the optimized S_1 excited states (see computational details in ESI) at the TDA-DFT level. The structured but very broad emission profiles together with the hole-electron analysis (displayed in Figure **6**) suggest an emission from both the ligand itself and a weakly MLCT state. The observation of emission associated with both the impym and bisphosphine ligands in both complexes (emission profiles of the ligands are shown in Figure **S3** in **ESI**) together with the broad emission spectrum is different from the characteristic photophysical behavior of many heteroleptic copper(I) complexes of the form $[Cu(N^N)(P^P)]^+$ that typically show broad charge-transfer emission,[35] and likewise is not consistent with our computations that predict a MLCT emission from both the S_1 and T_1 excited states (Cu -> N^N MLCT). In order to rationalize the unusual emission profile of the complexes, we first investigated the solution-state stability by

^{1}H NMR. In DCM under photoexcitation no chemical decomposition was observed. Tetraphenylethene (TPE) derivatives, well-known to display AIE, showed similarly weaker and blue-shifted emission in dilute solution in good solvents compared with aggregated samples.[36] This led us to hypothesise that under dilute DCM conditions, the CT state is weakly emissive, but that it could be turned on in an aggregated state, which suppresses non-radiative decay, by addition of an anti-solvent.

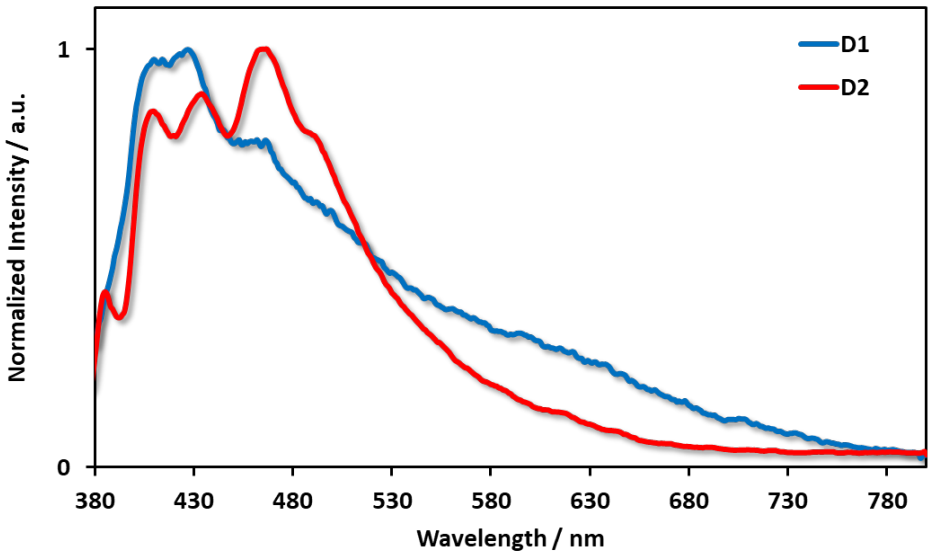

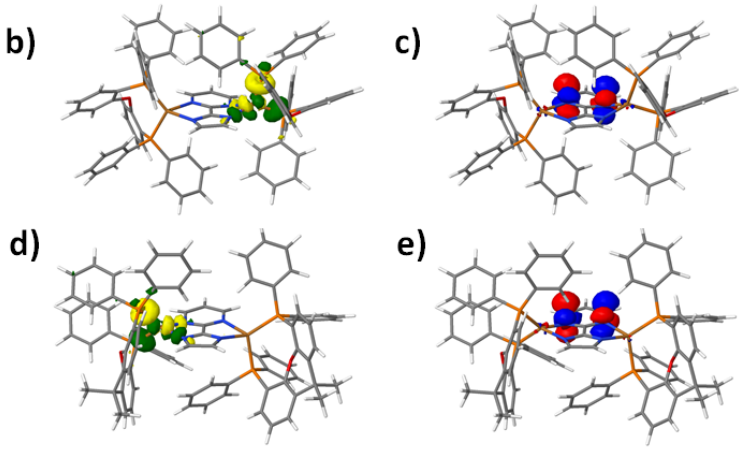

Figure **6**. (a) Photoluminescence spectra of **D1** and **D2** in deaerated DCM at room temperature. λ_{exc} = 360 nm. Hole [electron] density isocontour plots for the optimized S_1 excited state of b) [d)] **D1** and c) [e)] **D2**.

We therefore investigated whether these complexes were AIE-active by promoting increasing aggregation in THF/DMSO solutions through addition of increasing water content; a 1:1 THF:DMSO solution (5×10^{-5} mol/mL) was used to mitigate against rapid precipitation and lack of control of uniform micro-suspensions (Figure **7**). Both complexes were found to be highly soluble in THF/DMSO (50:50) solution (solubility > 50 mg/mL) but are insoluble in water (solubility < 0.2 mg/mL). Samples with 10 – 40% v/v water to 1:1 THF:DMSO showed weak LC emission at ~440 nm, close to what was observed for the emission of DCM solutions. With the addition of increasing water content over this range, the solubility of both complexes continuously decreased and micro-suspensions formed, which was linked to a decrease in the intensity of the high-energy emission and the appearance of a red-shifted, broad emission band that we assigned to a MLCT emission, which is now consistent with the predicted S_1 excited state energy. For both complexes, AIE could be turned on with greater than 50% water content. Emission could be enhanced as much as tenfold for **D1** and 39-fold for **D2**; however, at very high water content (90% water for **D1** and 80% water for **D2**), emission began to be quenched. Accompanying the emission enhancement was an unusual red-shift in the emission, the difference of λ_{PL} of emission before and after aggregation is 110 nm for **D1** and 138 nm for **D2**. Strong intermolecular interactions of tetrahedral copper(I) complexes leading to excimer emission are exceedingly rare and thus the large red-shift in emission profile after aggregation is very likely not due to intermolecular interactions between the copper(I) complexes.

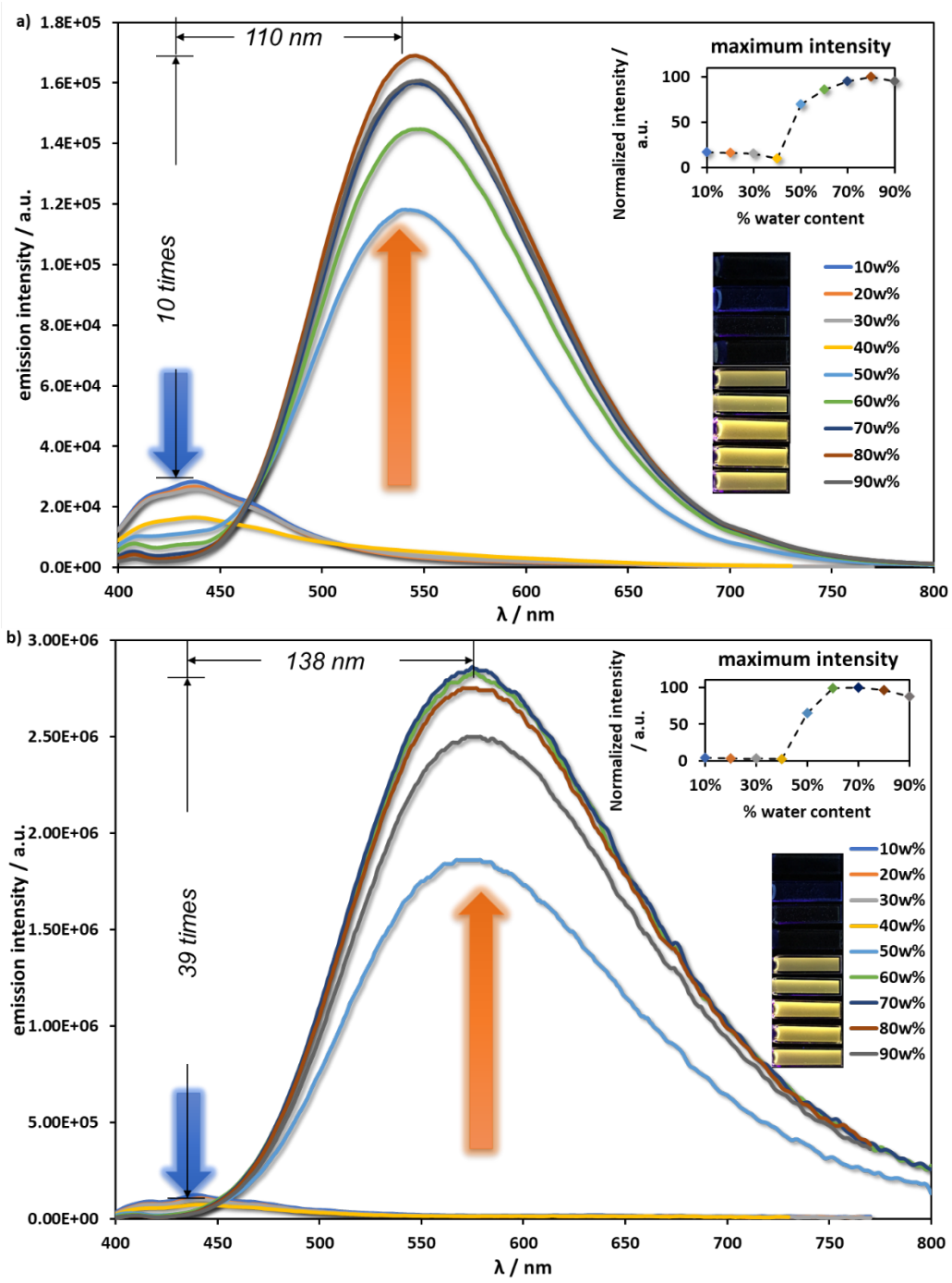

Figure **7**. Emission spectra of a) **D1** and b) **D2**, measured in THF/DMSO/water (water concentration from 10% to 90%) with consistent sample loading; solution samples were not degassed. λ_{exc} = 360 nm.

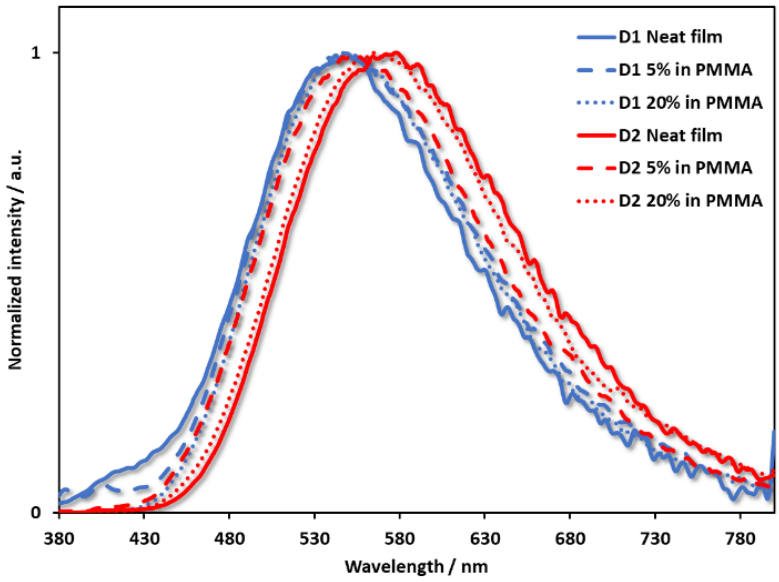

Figure **8**. Photoluminescence spectra of **D1** and **D2** in neat film (solid), 5 wt% in PMMA doped film (dash) and 20 wt% in PMMA doped film (dot). λ_{exc} = 360 nm.

We next turned our attention to understanding the photophysics of **D1** and **D2** in the solid state, in part to interrogate the mechanism underpinning the observations in our AIE studies. We investigated the photophysics of spin-coated neat films of **D1** and **D2**, as well as PMMA doped films at 5 wt% and 20 wt% (Figure **8**). The photophysical data are compiled in Table **4**. Both complexes are green-to-yellow emitters with emission maxima modestly red-shifted in neat films compared to doped films. The spectra in all cases remained broad and unstructured, indicative of emission from a CT excited state, whereas TDA-DFT calculations pointed to a MLCT state from the Cu centre to the impym ligand. The similar energies and profiles in the solid state compared to the emission observed in a poor solvent (THF/DMSO/water 10%/10%/80%) supports our hypothesis that in organic solutions, the non-radiative decay channels from this state are severe, and only the weak LC emission from the bridging ligand and bisphosphine ligands becomes apparent. By contrast, the AIE-displaying copper(I) systems reported by Li *et al*. (Figure **9a**) showed almost no spectral change but did show a large intensity

enhancement with increasing water content.[16] Moreover, AIE was not observed for thin-film samples, which is different from that observed by Bryce *et al*, where they found a large difference in the energies of the triplet excited states (Figure **9b**) in the doped or neat films.[37]

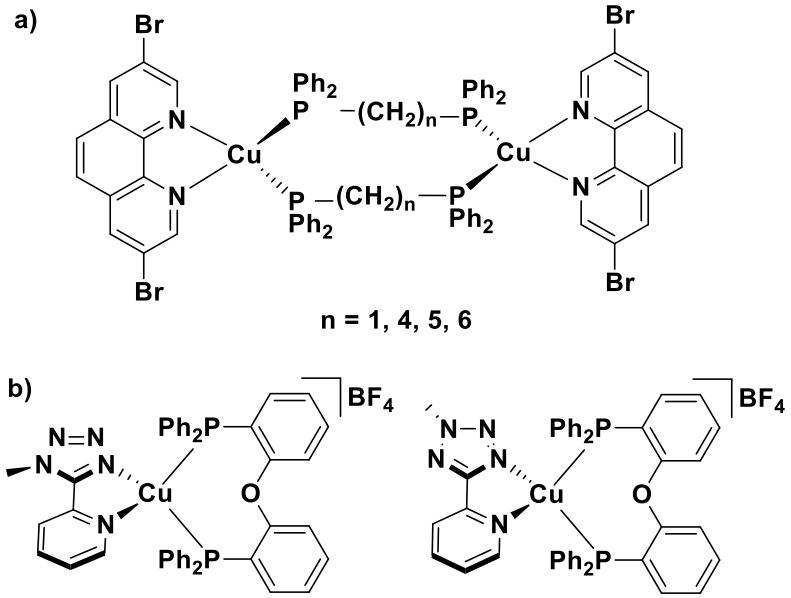

Figure **9**. a) AIE dinuclear copper(I) complexes reported by Li *et al*.,[16] b) AIE-TADF copper(I) complexes reported by Bryce *et al*.[37]

Table **4**. Thin film photophysics of **D1** and **D2**.

Complex	Conditions[a]	λ_{PL} / nm[b]	τ_{PL} / ns[c]	Φ_{PL} / %[d]
D1	Neat film	552	349(12%); 1277(44%); 3760(44%)	5
	5 wt% in PMMA	545	686(13%); 2676(49%); 8434(38%)	9
	20 wt% in PMMA	539	662(17%); 2588(51%); 7623((32%)	8
D2	Neat film	577	557(23%); 1856(57%); 5447(20%)	4
	5 wt% in PMMA	569	574(17%); 2299(50%); 8685(33%)	6
	20 wt% in PMMA	554	604(16%); 2286(52%); 8243(32%)	6

[a] Spin-coated from chloroform solution; [b] under vacuum, λ_{exc} = 360 nm; [c] under vacuum, λ_{exc} = 379 nm, weights are placed in parenthesis; [d] Φ_{PL}s measured under deaerated condition, λ_{exc} = 360 nm.

The crystalline powder samples of **D2** were found to be especially emissive compared to the solution or thin film samples. Although the packing and solvation of crystals may change during handling and degassing samples, the emission color observed was still found to be strongly dependent on the crystallization conditions. All spectra are broad and unstructured, which is indicative of a CT state (Figure **10**). The photophysical data are summarized in Table **5**. For **D1**, despite numerous crystallisation conditions tried, only one conformation was observed, and there was no notable difference in the photophysics for samples prepared using different crystallisation conditions. The three crystalline samples showed bluish green (CIE plot is shown in Figure **S4** in **ESI**) to greenish-yellow emission. Crystals of **D2-a** showed a λ_{PL} of 530 nm and the highest Φ_{PL} (46%) of the three samples. The crystals of **D1** were found to be weakly yellow-emissive with a λ_{PL} of 540 nm (Φ_{PL} = 4%) while the yellow-emissive **D2-b** crystals (λ_{PL} of 568 nm) showed an intermediate Φ_{PL} of 30%. Noteworthy is the significant energy difference of the emission between

pseudopolymorphic crystals of **D2** (ΔE = 140 meV). Aerated samples of **D1** exhibited a bi-exponential decay at room temperature [τ_{PL} = 0.4 (47%) 1.4 (53%) μs τ_{avg} = 0.93 μs] while deaerated sample showed a tri-exponential decay [τ_{PL} = 0.2 (17%) 0.8 (53%) 3.0 (30%) μs τ_{avg} = 1.36 μs]. Hence there are accessible triplet excited states involved in the emission process. Both deaerated (under vacuum) and aerated **D2-a** crystals exhibited multi-exponential decay. The τ_{PL} of **D2-a** crystals is very sensitive to oxygen, with deaerated samples showing τ_{PL} = 3.7 (1%) 26.8 (5%) 137.3 (94%) μs (τ_{avg} = 130.44 μs) while aerated samples showed much shorter τ_{PL} = 0.8 (4%) 3.0 (20%) 9.9 (62%) 30.3 (13%) μs (τ_{avg} = 10.68 μs). Similarly, **D2-b** crystals showed tri-exponential decay with emission strongly quenched in the presence of oxygen [τ_{PL} = 0.3(14%) 1.8(17%) 9.8(69%) μs (τ_{avg} = 7.11 μs) for aerated samples and τ_{PL} = 0.8(2%) 7.9(33%) 35.1(64%) μs (τ_{avg} = 25.09 μs) for deaerated samples]. According to the TDA-DFT calculations of the crystal structures of **D2-a** and **D2-b** there is only a 31 meV difference in their lowest triplet excited state energies. We thus believe that the observed difference in emission between **D2-a** and **D2-b** results from a combination of differences in solvation and pseudopolymorphism resulting from differences in the conformation of the two samples.

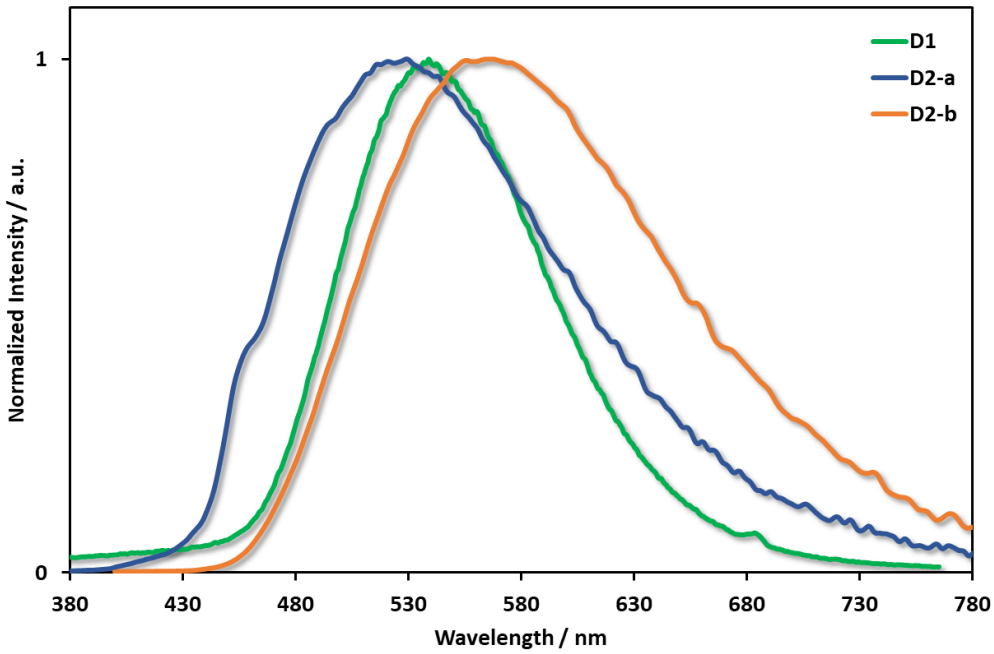

Figure **10**. Steady-state PL spectra of **D1**, **D2-a** and **D2-b** crystals at room temperature. λ_{exc} = 360 nm.

There are now numerous reports of mononuclear copper complexes that emit via a TADF mechanism. TADF in these complexes is made possible due to the presence of MLCT singlet and triplet excited states that lead to a small exchange integral between the excited states and a correspondingly small ΔE_{ST}, the energy difference between the first excited singlet and triplet states.[35,38] In order to assess whether **D1** and **D2** also emit via TADF we conducted time-resolved emission spectroscopy (TRES) at 77 K (Figure **11**) on crystalline samples. For **D1** (Figure **11a**), a very weak prompt fluorescence at λ_{PL} of 485 nm and a bright delayed phosphorescence at λ_{PL} of 570 nm were observed, corresponding to a ΔE_{ST} of 0.40 eV, which is in good agreement with the 0.3 eV predicted ΔE_{ST} at the TDA-DFT level (Table **5**). The measured ΔE_{ST} is larger than that in most of the purely organic TADF

materials[39] and Cu(I) complexes [0.12 eV for $[Cu(dmp)(phanephos)]^+$,[40] and 0.08 eV for $Cu(DPEPhos)(pz_2Bph_2)$];[41] and can be understood on the basis of the weakly MLCT character observed for the S_1 excited states of both compounds. In spite of this large ΔE_{ST}, as shown in Figure **S1**, the temperature-dependent time-resolved PL decay study shows that the emission on the microsecond timescale is still weakly thermally activated, implying that TADF is still operating in **D1**. Another plausible interpretation of the photophysical data is that the emission at 485 nm originates from an LC state.

Crystals of **D2-a** and **D2-b** behaved in a similar manner in their TRES measurements; both show prompt emission profiles (time window: 10-100 ns) of very similar energy to their delayed emission profiles (time window: 0.1-1 ms) at low temperature (Figure**s 11b** & **c**). These latter emission spectra were, respectively, 0.25 eV and 0.41 eV blue-shifted compared to their room temperature steady-state emission spectra. We attribute this shift to an inability of co-crystallized solvent molecules to reorganize to stabilize the transition dipole moment of the emitter in the crystal; this effect has been observed previously for multinuclear gold(I) complexes,[42] TDA-DFT calculations predict ΔE_{ST} values of 0.42 and 0.43 eV for **D2-b** and **D2-a**, respectively, which implies that TADF would play an even smaller role in **D2**, and that phosphorescence would be the dominant contribution to the delayed emission. The corresponding experimental result can be seen in the temperature-dependent PL decay of **D2-a**. As shown in Figure **S2**, the contribution of the delayed emission was dramatically enhanced when the temperature decreased from 295 K to 225 K, implying that suppressing thermal vibration can effectively enhance the triplet contribution. Furthermore, the delayed emission increased with decreasing temperature,

which further confirms that phosphorescence is dominant in the delayed emission at long time below 225 K.

Table **5**. Photophysical data for crystalline samples of **D1** and **D2**

	λ_{PL}[a] / nm	λ_{PL}[b] / nm	λ_{PL}[c] / nm	Φ_{PL}[d] / %	τ_{PL}[e] / μs	τ_{PL}[f] / μs	ΔE_{ST}[g] / eV	ΔE_{ST}[h] / eV
D1	540	485	570	4	0.4 (47%);1.4 (53%)	0.2(17%);0.8(53%);3.0(30%)	0.40	0.30
D2-a	530	490	490	46	0.8(4%);3.0 (20%);9.9(62%);30.3(13%)	3.7 (1%);26.8 (5%);137.3 (94%)	N/A	0.45
D2-b	568	503	487	30	0.3(14%);1.8(17%);9.8(69%)	0.8(2%);7.9(33%);35.1(64%)	N/A	0.43

[a] Steady-state emission at 298 K. λ_{exc} = 360 nm; [b] prompt emission at 77 K. Time window: 1 – 100 ns. λ_{exc} = 360 nm; [c] delayed emission at 77 K. Time window: 0.1 – 1 ms. λ_{exc} = 360 nm; [d] under N_2 at 298 K. λ_{exc} = 360 nm; [e] aerated samples at 298 K. λ_{exc} = 378 nm; [f] deaerated samples at 298 K. λ_{exc} = 378 nm; [g] experimentally determined from the onsets of the prompt emission and delayed emission; [h] determined from the TD-DFT calculations.

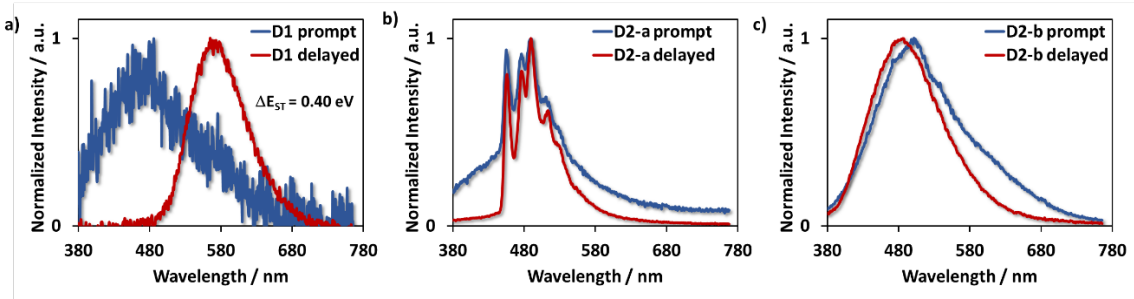

Figure **11**. TRES measurement results of a) **D1**, b) **D2-a** and c) **D2-b** at 77 K in the crystalline sample. The emission spectra collected in the 1-100 ns time window were used for the prompt emission profile, while the emission spectra collected in the 0.1-1 ms time window were used for the delayed emission profile to capture phosphorescence. Spectrometer: time-gated intensified CCD. Excitation source: 343 nm femto-second laser.

The different photophysical behaviour of the two pseudopolymorphs of **D2** motivated us to investigate the mechanochromic properties of the two complexes (Figure **12**). The crystals of **D1** and **D2-a** show λ_{PL} of 540 and 530 nm, respectively, and Φ_{PL} of 4% and 46%, respectively; crystals of **D2-b** show λ_{PL} of 568 nm. For **D1** and **D2-a**, emission in both samples is red-shifted and somewhat quenched upon grinding, while for **D2-b** no remarkable difference was observed upon grinding. The PL spectrum and Φ_{PL} of **D2-a** (λ_{PL} = 567 nm, Φ_{PL} = 33%) post grinding are in good agreement with the data for **D2-b**.

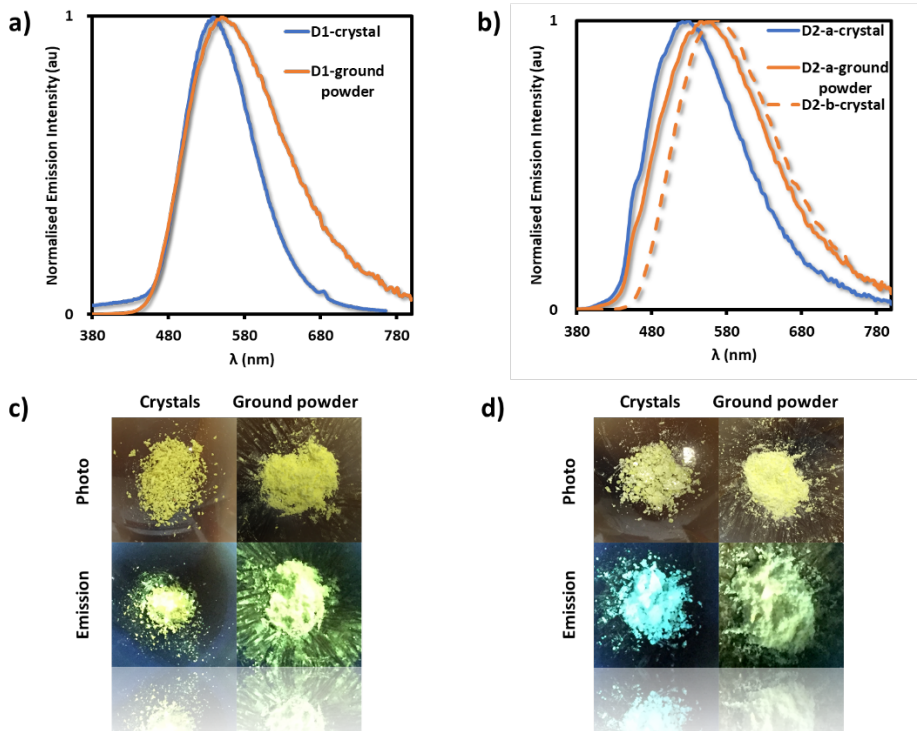

Figure **12**. a) PL spectra of fresh crystals and ground powder of **D1**. λ_{exc} = 360 nm; b) PL spectra of fresh crystals and ground powder of **D2-a**. λ_{exc} = 360 nm; c) photos of crystals and ground powders of **D1** with and without UV light irradiation (λ_{exc} = 365 nm); d) photos

of crystals and ground powders of **D2-a** with and without UV light irradiation (λ_{exc} = 365 nm).

Although there are only a few studies of mechanochromic luminescence for mono or dinuclear copper(I) complexes, both examples being related to BF_4 coordination to a linear $[Cu(NHC)_2]BF_4$ complex,[43,44] it has been well studied for copper(I) halide clusters.[45,46] For instance, the $[Cu_4I_4(PPh_2(CH_2CH{=}CH_2))_4]$ cluster reported by Boilot *et al*. exhibited a red-shift of 0.2 eV (530 nm for crystal and 580 nm for ground powder) after grinding the crystals; a significant enhancement in the emission intensity was also observed. They attributed the color change to a change in intracluster Cu···Cu distance in the two samples and emission resulting from two different states (MLCT and metal-metal-to-ligand charge transfer, MMLCT).[47] Zhang *et al*. reported a chiral C_3-symmetric cubane cluster, $[Cu_4I_4(TMP)_4]$, that showed a color change from green to yellow. The change in color was ascribed by the authors to a change in weak intermolecular interactions, and possibly a change in solvent molecules present in the crystal structure upon grinding.[48] Unlike the first aforementioned literature example, the Cu···Cu distances observed in the crystal structures of **D1** and **D2** are much larger than what is required for a possible metal-metal interaction that leads to an MMLCT state. Based on the observed photophysical properties of the crystals and the TDA-DFT calculations, we speculate that changes in solvation and weak intermolecular interactions, as well as conformation are the primary contributing factors to the observed changes in the emission upon grinding.

Conclusions and outlook

Two heteroleptic dinuclear copper(I) complexes bearing a bridging imidazolylpyrimidine ligand were synthesised and characterized. Both complexes showed a very negative excited-state oxidation potential (-1.85 V for **D1** and -1.75 V for **D2**), a modestly positive excited-state reduction potential (0.65 V for **D1**, 0.69 V for **D2**) and a very negative ground state reduction potential (-2.20 V for **D1**, -2.16 V for **D2**). Although the lack of visible light absorption might be a disadvantage, these dinuclear copper(I) complexes are likely to be an earth-abundant alternative to the well-studied photoreductant, *fac*-Ir(ppy)$_3$.

Both complexes showed aggregation-induced emission in THF/DMSO/water solutions, the after-aggregation samples exhibited intense and red-shifted compared to the homogeneous dilute solution samples. The TADF properties of these two complexes were studied via both temperature-dependent PL decay measurements and TRES. Although complex **D1** has a large ΔE_{ST} of 0.40 eV, its TADF behaviour can still be observed through its temperature-dependent PL decay curves. TDA-DFT results showed that both polymorphs of complex **D2** have even larger ΔE_{ST}s. The temperature-dependent PL decay measurement of the **D2-a** crystals shows phosphorescence is dominant at long times when the temperature is below 225 K. Grinding of **D2-a** crystals resulted in a red-shifted and attenuated emission, and we speculated this red-shift has resulted from a combined effect of changes in solvation and conformational change of the P^P ligand of the complex.

ASSOCIATED CONTENT

Supporting Information.

^{1}H NMR, ^{13}C NMR, 19F NMR and ^{31}P NMR of all new compounds; supplementary characterization data; supplementary computational data and coordinates; supplementary photophysical and electrochemical data.

ACKNOWLEDGMENT

C. Li thanks the Prof. & Mrs. Purdie Bequests Scholarship and AstraZeneca for a PhD Studentship. We are grateful to the Engineering and Physical Sciences Research Council of the UK (EPSRC) for financial support (grants EP/R035164/1 and EP/P010482/1). We acknowledge the EPSRC UK National Mass Spectrometry Facility at Swansea University for mass spectrometry analysis. The work in Mons was supported by the European Commission / Région Wallonne (FEDER – BIORGEL project), the Consortium des Équipements de Calcul Intensif (CÉCI), funded by the Fonds National de la Recherche Scientifique (F.R.S.-FNRS) under Grant No. 2.5020.11 as well as the Tier-1 supercomputer of the Fédération Wallonie-Bruxelles, infrastructure funded by the Walloon Region under Grant Agreement n1117545, and FRS-FNRS.

References

(1) WebElements Periodic Table » Periodicity » Abundance in Earth's crust (by weight) » Periodic table gallery https://www.webelements.com/periodicity/abund_crust/ (accessed Feb 6, 2020).

(2) Sakaki, S.; Mizutani, H.; Kase, Y. I.; Inokuchi, K. J.; Arai, T.; Hamada, T. Photoinduced Electron Transfer between [Cu(Dmphen)L2]+ [Dmphen = 2,9-Dimethyl-1,10-Phenanthroline, L = PPhn(C6H4OMe-p)3-n (n = 0-3)] and Methyl

Viologen. *J. Chem. Soc. - Dalt. Trans.* **1996**, No. 9, 1909–1914. https://doi.org/10.1039/DT9960001909.

(3) Sakaki, S.; Mizutani, H.; Kase, Y. ichi; Arai, T.; Hamada, T. Photoinduced Electron Transfer Reaction between [Cu(Dmp)P2]+or- (P=PPh3 or PPh2(m-C6H4SO3-) and Viologen Derivatives. *Inorganica Chim. Acta* **1994**, *225* (1–2), 261–267. https://doi.org/10.1016/0020-1693(94)04056-7.

(4) Meyer, M.; Albrecht-Gary, A. M.; Dietrich-Buchecker, C. O.; Sauvage, J. P. π-π Stacking-Induced Cooperativity in Copper(I) Complexes with Phenanthroline Ligands. *Inorg. Chem.* **1999**, *38* (10), 2279–2287. https://doi.org/10.1021/ic981259+.

(5) Cuttell, D. G.; Kuang, S. M.; Fanwick, P. E.; McMillin, D. R.; Walton, R. A. Simple Cu(I) Complexes with Unprecedented Excited-State Lifetimes. *J. Am. Chem. Soc.* **2002**, *124* (1), 6–7. https://doi.org/10.1021/ja012247h.

(6) Zhang, Q.; Zhou, Q.; Cheng, Y.; Wang, L.; Ma, D.; Jing, X.; Wang, F. Highly Efficient Green Phosphorescent Organic Light-Emitting Diodes Based on CuI Complexes. *Adv. Mater.* **2004**, *16* (5), 432–436. https://doi.org/10.1002/adma.200306414.

(7) Xiao, P.; Dumur, F.; Zhang, J.; Fouassier, J. P.; Gigmes, D.; Lalevée, J. Copper Complexes in Radical Photoinitiating Systems: Applications to Free Radical and Cationic Polymerization upon Visible Leds. *Macromolecules* **2014**, *47* (12), 3837–3844. https://doi.org/10.1021/ma5006793.

(8) Harkins, S. B.; Peters, J. C. A Highly Emissive Cu2N2 Diamond Core Complex Supported by a [PNP]- Ligand. *J. Am. Chem. Soc.* **2005**, *127* (7), 2030–2031.

https://doi.org/10.1021/ja043092r.

(9) Linfoot, C. L.; Richardson, P.; Hewat, T. E.; Moudam, O.; Forde, M. M.; Collins, A.; White, F.; Robertson, N. Substituted [Cu(I)(POP)(Bipyridyl)] and Related Complexes: Synthesis, Structure, Properties and Applications to Dye-Sensitised Solar Cells. *Dalt. Trans.* **2010**, *39* (38), 8945–8956. https://doi.org/10.1039/c0dt00190b.

(10) Zink, D. M.; Volz, D.; Baumann, T.; Mydlak, M.; Flügge, H.; Friedrichs, J.; Nieger, M.; Bräse, S. Heteroleptic, Dinuclear Copper(i) Complexes for Application in Organic Light-Emitting Diodes. *Chem. Mater.* **2013**, *25* (22), 4471–4486. https://doi.org/10.1021/cm4018375.

(11) Volz, D.; Chen, Y.; Wallesch, M.; Liu, R.; Fléchon, C.; Zink, D. M.; Friedrichs, J.; Flügge, H.; Steininger, R.; Göttlicher, J.; Heske, C.; Weinhardt, L.; Bräse, S.; So, F.; Baumann, T. Bridging the Efficiency Gap: Fully Bridged Dinuclear Cu(I)-Complexes for Singlet Harvesting in High-Efficiency OLEDs. *Adv. Mater.* **2015**, *27* (15), 2538–2543. https://doi.org/10.1002/adma.201405897.

(12) Bizzarri, C.; Strabler, C.; Prock, J.; Trettenbrein, B.; Ruggenthaler, M.; Yang, C. H.; Polo, F.; Iordache, A.; Brüggeller, P.; De Cola, L. Luminescent Dinuclear Cu(I) Complexes Containing Rigid Tetraphosphine Ligands. *Inorg. Chem.* **2014**, *53* (20), 10944–10951. https://doi.org/10.1021/ic5012204.

(13) Kobayashi, A.; Hasegawa, T.; Yoshida, M.; Kato, M. Environmentally Friendly Mechanochemical Syntheses and Conversions of Highly Luminescent Cu(I) Dinuclear Complexes. *Inorg. Chem.* **2016**, *55* (5), 1978–1985. https://doi.org/10.1021/acs.inorgchem.5b02160.

(14) Lin, L.; Chen, D. H.; Yu, R.; Chen, X. L.; Zhu, W. J.; Liang, D.; Chang, J. F.; Zhang, Q.; Lu, C. Z. Photo- and Electro-Luminescence of Three TADF Binuclear Cu(i) Complexes with Functional Tetraimine Ligands. *J. Mater. Chem. C* **2017**, *5* (18), 4495–4504. https://doi.org/10.1039/c7tc00443e.

(15) Schinabeck, A.; Chen, J.; Kang, L.; Teng, T.; Homeier, H. H. H.; Suleymanova, A. F.; Shafikov, M. Z.; Yu, R.; Lu, C.-Z.; Yersin, H. Symmetry-Based Design Strategy for Unprecedentedly Fast Decaying Thermally Activated Delayed Fluorescence (TADF). Application to Dinuclear Cu(I) Compounds. *Chem. Mater.* **2019**, *31* (12), 4392–4404. https://doi.org/10.1021/acs.chemmater.9b00671.

(16) Xin, X. L.; Chen, M.; Ai, Y. B.; Yang, F. L.; Li, X. L.; Li, F. Aggregation-Induced Emissive Copper(I) Complexes for Living Cell Imaging. *Inorg. Chem.* **2014**, *53* (6), 2922–2931. https://doi.org/10.1021/ic402685u.

(17) Carrara, S.; Aliprandi, A.; Hogan, C. F.; De Cola, L. Aggregation-Induced Electrochemiluminescence of Platinum(II) Complexes. *J. Am. Chem. Soc.* **2017**, *139* (41), 14605–14610. https://doi.org/10.1021/jacs.7b07710.

(18) Kalinowski, J.; Fattori, V.; Cocchi, M.; Williams, J. A. G. Light-Emitting Devices Based on Organometallic Platinum Complexes as Emitters. *Coord. Chem. Rev.* **2011**, *255* (21–22), 2401–2425. https://doi.org/10.1016/j.ccr.2011.01.049.

(19) Voss, M. E.; Beer, C. M.; Mitchell, S. A.; Blomgren, P. A.; Zhichkin, P. E. A Simple and Convenient One-Pot Method for the Preparation of Heteroaryl-2-Imidazoles from Nitriles. *Tetrahedron* **2008**, *64* (4), 645–651. https://doi.org/10.1016/j.tet.2007.11.009.

(20) Bergmann, L.; Friedrichs, J.; Mydlak, M.; Baumann, T.; Nieger, M.; Bräse, S.

Outstanding Luminescence from Neutral Copper(i) Complexes with Pyridyl-Tetrazolate and Phosphine Ligands. *Chem. Commun.* **2013**, *49* (58), 6501–6503. https://doi.org/10.1039/c3cc42280a.

(21) Moral, M.; Muccioli, L.; Son, W. J.; Olivier, Y.; Sancho-Garcia, J. C. Theoretical Rationalization of the Singlet-Triplet Gap in Oleds Materials: Impact of Charge-Transfer Character. *J. Chem. Theory Comput.* **2015**, *11* (1), 168–177. https://doi.org/10.1021/ct500957s.

(22) Jmol: an open-source Java viewer for chemical structures in 3D, http://www.jmol.org.

(23) Kavarnos, G. J.; Turro, N. J. Photosensitization by Reversible Electron Transfer: Theories, Experimental Evidence, and Examples. *Chem. Rev.* **1986**, *86* (2), 401–449. https://doi.org/10.1021/cr00072a005.

(24) Larsen, C. B.; Wenger, O. S. Photoredox Catalysis with Metal Complexes Made from Earth-Abundant Elements. *Chem. - A Eur. J.* **2018**, *24* (9), 2039–2058. https://doi.org/10.1002/chem.201703602.

(25) Hockin, B. M.; Li, C.; Robertson, N.; Zysman-Colman, E. Photoredox Catalysts Based on Earth-Abundant Metal Complexes. *Catal. Sci. Technol.* **2019**, *9* (4), 889–915. https://doi.org/10.1039/c8cy02336k.

(26) Gao, H.; Xia, S.; Zhang, R.; Zhao, Y.; Wang, W.; An, Z.; Qi, H. Efficient Green Electrogenerated Chemiluminescence from Cyclometalated Iridium(III) Complex. *J. Electroanal. Chem.* **2015**, *755* (6), 71–76. https://doi.org/10.1016/j.jelechem.2015.07.026.

(27) Kern, J. M.; Sauvage, J. P. Photoassisted C-C Coupling via Electron Transfer to

Benzylic Halides by a Bis(Di-Imine) Copper(I) Complex. *J. Chem. Soc. Chem. Commun*. **1987**, No. 8, 546–548. https://doi.org/10.1039/C39870000546.

(28) Zhang, Y.; Traber, P.; Zedler, L.; Kupfer, S.; Gräfe, S.; Schulz, M.; Frey, W.; Karnahl, M.; Dietzek, B. Cu(i): Vs. Ru(II) Photosensitizers: Elucidation of Electron Transfer Processes within a Series of Structurally Related Complexes Containing an Extended π-System. *Phys. Chem. Chem. Phys*. **2018**, *20* (38), 24843–24857. https://doi.org/10.1039/c8cp04595j.

(29) Zhang, Y.; Heberle, M.; Wächtler, M.; Karnahl, M.; Dietzek, B. Determination of Side Products in the Photocatalytic Generation of Hydrogen with Copper Photosensitizers by Resonance Raman Spectroelectrochemistry. *RSC Adv*. **2016**, *6* (107), 105801–105805. https://doi.org/10.1039/c6ra21469j.

(30) Teegardin, K.; Day, J. I.; Chan, J.; Weaver, J. Advances in Photocatalysis: A Microreview of Visible Light Mediated Ruthenium and Iridium Catalyzed Organic Transformations. *Org. Process Res. Dev*. **2016**, *20* (7), 1156–1163. https://doi.org/10.1021/acs.oprd.6b00101.

(31) Roth, H. G.; Romero, N. A.; Nicewicz, D. A. Experimental and Calculated Electrochemical Potentials of Common Organic Molecules for Applications to Single-Electron Redox Chemistry. *Synlett* **2016**, *27* (5), 714–723. https://doi.org/10.1055/s-0035-1561297.

(32) Cardona, C. M.; Li, W.; Kaifer, A. E.; Stockdale, D.; Bazan, G. C. Electrochemical Considerations for Determining Absolute Frontier Orbital Energy Levels of Conjugated Polymers for Solar Cell Applications. *Adv. Mater*. **2011**, *23* (20), 2367–2371. https://doi.org/10.1002/adma.201004554.

(33) Rehm, D.; Weller, A. Kinetics of Fluorescence Quenching by Electron and H-Atom Transfer. *Isr. J. Chem.* **1970**, *8* (2), 259–271. https://doi.org/10.1002/ijch.197000029.

(34) Braslavsky, S. E. Glossary of Terms Used in Photochemistry 3rd Edition: (IUPAC Recommendations 2006). *Pure Appl. Chem.* **2007**, *79* (3), 293–465. https://doi.org/10.1351/pac200779030293.

(35) Czerwieniec, R.; Leitl, M. J.; Homeier, H. H. H.; Yersin, H. Cu(I) Complexes – Thermally Activated Delayed Fluorescence. Photophysical Approach and Material Design. *Coord. Chem. Rev.* **2016**, *325*, 2–28. https://doi.org/10.1016/j.ccr.2016.06.016.

(36) Dong, Y.; Lam, J. W. Y.; Qin, A.; Liu, J.; Li, Z.; Tang, B. Z.; Sun, J.; Kwok, H. S. Aggregation-Induced Emissions of Tetraphenylethene Derivatives and Their Utilities as Chemical Vapor Sensors and in Organic Light-Emitting Diodes. *Appl. Phys. Lett.* **2007**, *91* (1), 011111. https://doi.org/10.1063/1.2753723.

(37) Li, G.; Nobuyasu, R. S.; Zhang, B.; Geng, Y.; Yao, B.; Xie, Z.; Zhu, D.; Shan, G.; Che, W.; Yan, L.; Su, Z.; Dias, F. B.; Bryce, M. R. Thermally Activated Delayed Fluorescence in CuI Complexes Originating from Restricted Molecular Vibrations. *Chem. - A Eur. J.* **2017**, *23* (49), 11761–11766. https://doi.org/10.1002/chem.201701862.

(38) Wong, M. Y.; Zysman-Colman, E. Purely Organic Thermally Activated Delayed Fluorescence Materials for Organic Light-Emitting Diodes. *Advanced Materials*. June 2017, p 1605444. https://doi.org/10.1002/adma.201605444.

(39) Liu, Y.; Li, C.; Ren, Z.; Yan, S.; Bryce, M. R. All-Organic Thermally Activated

Delayed Fluorescence Materials for Organic Light-Emitting Diodes. *Nat. Rev. Mater.* **2018**, *3* (22), 1605444. https://doi.org/10.1038/natrevmats.2018.20.

(40) Czerwieniec, R.; Kowalski, K.; Yersin, H. Highly Efficient Thermally Activated Fluorescence of a New Rigid Cu(i) Complex [Cu(Dmp)(Phanephos)]+. *J. Chem. Soc. Dalt. Trans.* **2013**, *42* (27), 9826–9830. https://doi.org/10.1039/c3dt51006a.

(41) Czerwieniec, R.; Yu, J.; Yersin, H. Blue-Light Emission of Cu(I) Complexes and Singlet Harvesting. *Inorg. Chem.* **2011**, *50* (17), 8293–8301. https://doi.org/10.1021/ic200811a.

(42) López-De-Luzuriaga, J. M.; Monge, M.; Olmos, M. E.; Quintana, J.; Rodríguez-Castillo, M. Stimuli-Responsive Solvatochromic Au(I)-Ag(I) Clusters: Reactivity and Photophysical Properties Induced by the Nature of the Solvent. *Inorg. Chem.* **2019**, *58* (2), 1501–1512. https://doi.org/10.1021/acs.inorgchem.8b03022.

(43) Hupp, B.; Nitsch, J.; Schmitt, T.; Bertermann, R.; Edkins, K.; Hirsch, F.; Fischer, I.; Auth, M.; Sperlich, A.; Steffen, A. Stimulus-Triggered Formation of an Anion–Cation Exciplex in Copper(I) Complexes as a Mechanism for Mechanochromic Phosphorescence. *Angew. Chemie - Int. Ed.* **2018**, *57* (41), 13671–13675. https://doi.org/10.1002/anie.201807768.

(44) Liske, A.; Wallbaum, L.; Hölzel, T.; Föller, J.; Gernert, M.; Hupp, B.; Ganter, C.; Marian, C. M.; Steffen, A. Cu-F Interactions between Cationic Linear N-Heterocyclic Carbene Copper(I) Pyridine Complexes and Their Counterions Greatly Enhance Blue Luminescence Efficiency. *Inorg. Chem.* **2019**, *58* (9), 5433–5445. https://doi.org/10.1021/acs.inorgchem.9b00337.

(45) Ford, P. C.; Cariati, E.; Bourassa, J. Photoluminescence Properties of Multinuclear

Copper(I) Compounds. *Chem. Rev.* **1999**, *99* (12), 3625–3647. https://doi.org/10.1021/cr960109i.

(46) Ford, P. C. Photochemical and Photophysical Studies of Tetranuclear Copper(I) Halide Clusters: An Overview. *Coord. Chem. Rev.* **1994**, *132* (C), 129–140. https://doi.org/10.1016/0010-8545(94)80032-4.

(47) Perruchas, S.; Goff, X. F. L.; Maron, S.; Maurin, I.; Guillen, F.; Garcia, A.; Gacoin, T.; Boilot, J. P. Mechanochromic and Thermochromic Luminescence of a Copper Iodide Cluster. *J. Am. Chem. Soc.* **2010**, *132* (32), 10967–10969. https://doi.org/10.1021/ja103431d.

(48) Yang, K.; Li, S. L.; Zhang, F. Q.; Zhang, X. M. Simultaneous Luminescent Thermochromism, Vapochromism, Solvatochromism, and Mechanochromism in a C3-Symmetric Cubane [Cu4I4P4] Cluster without Cu-Cu Interaction. *Inorg. Chem.* **2016**, *55* (15), 7323–7325. https://doi.org/10.1021/acs.inorgchem.6b00922.

TOC (For Table of Contents Only)

The synthesis and the photophysical study of two dinuclear copper(I) complexes bearing a 2-(1*H*-imidazol-2-yl)pyrimidine bridging ligand are described. Temperature-dependant photophysical studies demonstrated emission through a combination of phosphorescence and thermally activated delayed fluorescence (TADF) for both complexes, and an intense emission (Φ_{PL} = 46%) was observed for a crystalline sample of one of the reported complexes. Two pseudopolymorphs of one of the dinuclear complex were isolated, and their photophysics is distinct.

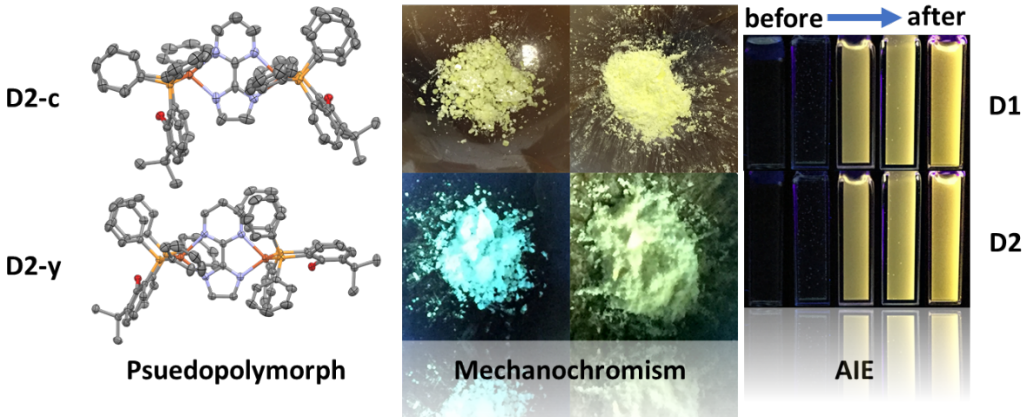
D2-c
D2-y
Psuedopolymorph
Mechanochromism
before
after
D1
D2
AIE